Influence of the Body on the Response of the Helmeted Head during Impact

Mazdak Ghajari[a], Ugo Galvanetto[b], Lorenzo Iannucci[a], Remy Willinger[c]

[a] *Imperial College London, Department of Aeronautics, South Kensington Campus, London SW7 2AZ, UK, m.ghajari@imperial.ac.uk*

[b] *University of Padova, Dipartimento di Costruzioni e Trasporti, Via Marzolo 9, 35131 Padova, Ital, galva@dic.unipd.it*

[c] *University of Strasbourg, UMR 7507 ULP-CNRS, 2 rue Boussingault, F67000, Strasbourg, France, remy.willinger@imfs.u-strasbg.fr*

Corresponding author: Mazdak Ghajari,
Email: m.ghajari@imperial.ac.uk,
Tel.: +44 796 4586225

Influence of the Body on the Response of the Helmeted Head during Impact

The most frequent type of injury that causes death or disability in motorcycle accidents is head injury. The only item of protective equipment that protects a motorcyclist's head in real-world accidents is the safety helmet. The protective capability of a helmet is assessed, according to international standards, through impact of a headform fitted with the helmet onto an anvil. The purpose of the present work was to study the influence of the presence of the body on the impact response of the helmeted head. Full-body and detached-head impacts were simulated using the Finite Element (FE) method. As a consequence of the presence of the body, the crushing distance of the helmet liner was drastically increased. This evidence indicated that the effect of the body should be included in impact absorption tests in order to provide conditions that are more realistic and stringent. The solution to an analytical model of the helmeted headform impact revealed that increasing the headform mass has the same influence on impact outputs, particularly the liner crushing distance, as including the whole body in impact tests. The added mass was calculated by using a helmeted Hybrid III dummy for an impact configuration frequently occurred in real-world accidents.

Keywords: helmets, impact absorption, drop tests, Hybrid III dummy, Finite Element method

Notation

$\|a\|$	resultant linear acceleration of the head
h	liner thickness
m	combined mass of helmet and headform
m_h	mass of head
y	central deflection of liner
E_L	longitudinal elastic modulus
E_T	transverse elastic modulus
F_h	contact force at the head/helmet interface
F_n	neck force
F_N	normal force at the helmet/anvil interface
G_{LT}	shear modulus
P_0	initial gas pressure
R	foam relative density, local radius of helmet exterior
$S_{uc,L}$	longitudinal compressive strength
$S_{uc,T}$	transverse compressive strength
$S_{ut,L}$	longitudinal tensile strength
$S_{ut,T}$	transverse tensile strength
V_0	impact velocity
$V_{0,r}$	reduced impact velocity
V_f	fibre volume fraction
t	time
α	ratio of total internal energy to internal energy of liner
γ_m	added mass index (ratio of the added mass to the original mass)
γ_u	ultimate shear strain
$\varepsilon_{uc,L}$	ultimate longitudinal compressive strain
$\varepsilon_{uc,T}$	ultimate transverse compressive strain
$\varepsilon_{ut,L}$	ultimate longitudinal tensile strain
$\varepsilon_{ut,T}$	ultimate transverse tensile strain
ν_{LT}	major Poisson ratio
ρ	density
σ_Y	yield stress
τ_u	shear strength
Δh	liner crushing distance

1. Introduction

Motorcyclists' safety is an important issue in transport policy because they are among the most vulnerable road users. Even though motorcycles comprise only 6.1% of all motorised vehicles in Europe (ACEM 2006), motorcyclists account for 16% of total road-user fatalities (COST327 2001). Head injury is the most frequent type of injuries which cause death or disability in motorcycle accidents. The only item of personal protective equipment that protects a motorcyclist's head in real world accidents is the safety helmet. Motorcycle helmets have to pass prescribed standard tests, prior to become commercially available, in order to assure that they have an acceptable protective capability.

A survey (Becker 1998) of the history of helmet standards revealed that the impact absorption test method has evolved considerably. The first standards adopted a simple method; the helmet was positioned on a fixed headform and impacted with a striker. Among the disadvantages of this method was using a fixed headform, while in real world accidents a moving head impacts another object. Current standards require dropping a helmeted headform on a rigid anvil at a specific impact velocity (Ghajari et al. 2008). The helmet passes the tests if the resultant linear acceleration of the headform ($|a(t)|$) is lower than a stated limit. For example, the UNECE 22.05 regulation (2002) requires dropping helmeted headforms at 7.5 m/s onto flat and kerbstone anvils. The pass/fail criteria are a 275 g peak linear acceleration and a value of 2400 for *HIC* (Head injury Criterion), which is defined as:

$$HIC = \max\{(t_2 - t_1)(\frac{1}{t_2 - t_1}\int_{t_1}^{t_2} |a(t)|\, dt)^{2.5}\}$$

where t_1 and t_2 are, respectively, any starting and ending time in impact pulse duration. It should be noted that the *HIC* has been criticised of having some

drawbacks (Kleiven 2006). Furthermore, there is a huge debate about its suitability for helmet standards (HIC-Workshop 2005). Although the impact absorption test method has been improved, it is still far from representing real world accidents, where the whole body is present. In fact, the probable consequences of excluding the rest of the body by employing a detached headform in drop tests have received little attention.

One way to investigate the effect of the body is to use anthropomorphic test dummies (COST327 2001, Gilchrist and Mills 1996, Tinard et al. 2009). In the COST action, which is probably the most recent study on the subject, a pedestrian Hybrid III dummy and its detached head were fitted with helmets and dropped onto flat anvils. Head linear acceleration was recorded during impacts and compared. It was concluded that "the effect of the body and the neck is thus a decrease of the measured linear acceleration values when compared with headform measurements", which implies that current test methods are conservative. The crushing distance of the helmet liner, however, was not reported and compared between dummy and headform drop tests. There is a possibility that in full-body tests the liner crushing distance increases and therefore, it is underestimated by using a detached headform. Hence, it is extremely important to determine the influence of the body on this impact output parameter.

In this paper, impacts of a helmeted Hybrid III and its helmeted head onto a flat anvil are simulated using the FE method. The results are compared considering both linear acceleration of the head and the crushing distance of the liner. A one-dimensional analytical model is proposed for the helmeted headform impact. The solution to this model reveals the relations between impact inputs, properties of the helmet and impact outputs. These relations are extremely important when the effect of

the body on impact outputs is to be included in headform drop tests, by modifying one or more impact inputs.

2. FE model of the helmet

A recently designed helmet, which is called AGV-T2 in this paper, was provided by Dainsese S.p.A. (a partner of the MYMOSA EU network) for drop tests. Size of the helmet was 57-58 cm. In spite of belonging to the AGV racers' range, this helmet is representative of a number of commercially available helmets, which have a composite shell and an Expanded Poly-Styrene (EPS) liner. In addition, the high energy absorption capability of the helmet reduced the risk of damaging the dummy in drop tests.

The main components of the AGV-T2 helmet are: the protective padding or liner, shell, chin strap, comfort padding and visor. The liner and shell are the components that absorb the impact energy; they were modelled as well as the chin strap. By contrast, the visor and comfort padding do not contribute to energy absorption and therefore they were not modelled.

EPS belongs to the category of closed-cell polymeric foams that collapse plastically when compressed beyond their elastic regime. Therefore, three regimes are distinguishable in its compressive stress-strain characteristic curve as shown in Figure 1. The first regime, which is linear elastic, is characterised by Young's modulus (E) and the Poisson ratio (v). Young's modulus of EPS is a function of its relative density (Gibson and Ashby 1999), while the Poisson ratio does not have a significant relation with the relative density. An investigation of the *crushable foam* material model of LS-DYNA (Hallquist 2007a), which was used for the liner, revealed that under a compressive load the Poisson ratio remains effective even beyond the elastic regime, while EPS does not deform laterally beyond this regime. Since the elastic regime is

negligible compared to the plateau regime, this constant was set to a very small value (0.01).

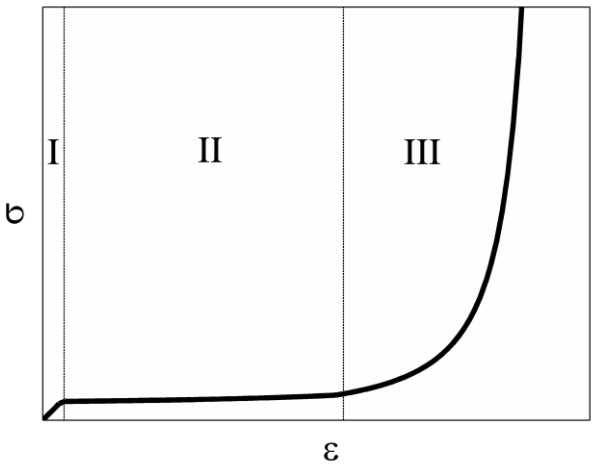

Figure 1 Typical engineering stress-engineering strain curve of EPS under compressive loading.

The plastic collapse of cells comprising the foam results in the long plateau of the curve depicted in Figure 1 (region II). This part of the curve can be fitted with (Mills and Gilchrist 2008):

$$\sigma = \sigma_Y + \frac{p_0 \varepsilon}{1 - \varepsilon - R} \tag{1}$$

where σ and ε are the compressive engineering stress and strain. σ_Y is the yield stress and p_0 is the initial gas pressure, which is usually equal to the atmospheric pressure (0.1 MPa). Experimental investigations (Gilchrist and Mills 1994) have shown that the yield stress can be described with:

$$\sigma_Y = CR^{1.5} \tag{2}$$

where C is a material constant. The quasi-static compression test data reported in (Di Landro et al. 2002) for EPS foams were used to calculate C. This constant was then increased by 20% to take into account the strain rate effect at helmet drop test speeds, as suggested by Mills et al. (2009). At the end, a value of 48.3 MPa was found for C.

Excessive compression of EPS causes cell walls to crush, which results in the steep rise of the stress when increasing the strain to a limiting strain. It forms the third part of the curve shown in Figure 1. This part of the curve is also a function of the relative density of the foam (Gibson and Ashby 1999).

In this work, the liner was modelled with the *crushable foam* material model of LS-DYNA (Hallquist 2007b). In this model, if the magnitudes of the principal stresses exceed the yield stress at each time step, they are scaled back to the yield surface. The unloading occurs on a line whose slope is equal to the Young modulus of the foam. The required inputs of this material model are presented in Table 1 for the foam parts of the helmet.

Table 1 Material properties of foam parts and chin strap

Part	ρ (kg/m^3)	E (MPa)	υ	σ_Y (MPa)
EPS top	20	2.9	0.01	0.13
EPS main	40	10.6	0.01	0.36
EPS cheek and chin	60	23.2	0.01	0.66
Chin strap	870	1000	0.3	-

The shell of the AGV-T2 helmet is made of a number of composite layers. According to the information provided by the helmet manufacturer, the constituents of these layers are Kevlar 49 fibres, carbon (T700) fibres, glass fibres and an epoxy resin. To obtain more information, six samples were cut from various regions of the shell. They were moulded in resin, polished and inspected under a microscope. The observations suggested that five different laminas are used in the shell: a Kevlar/carbon/epoxy hybrid unidirectional (UD) lamina, a glass/epoxy twill weave woven lamina, a glass/epoxy UD lamina, a polymer fibre/epoxy plain weave woven lamina and a carbon/epoxy UD lamina. Further investigation of the microscopy images provided approximate thicknesses and fibre volume fractions of the laminas as

well as lay-up of the shell at different regions. Given the constituents of the layers and volume fractions, the mechanical properties of the layers were either found in open literature or obtained from the rule of mixtures, Halpin-Tsai equations and assuming simple failure mechanisms, as are completely explained in (Agarwal et al. 2006) and summarised in (Cernicchi et al. 2008). For instance, the mechanical properties of the glass/epoxy UD lamina are given in Table 2. The properties of the other laminae are not provided for confidentiality reasons.

Table 2 Mechanical properties of the glass/epoxy UD lamina

	(V_f = 0.6) (Soden et al. 1998)
$\rho(kg/m^3)$	1984
E_L *(GPa)*	46
E_T *(GPa)*	16
G_{LT} *(GPa)*	5.8
ν_{LT}	0.28
$S_{ut,L}$ *(MPa)*	1280
$\varepsilon_{ut,L}$	0.028
$S_{uc,L}$ *(MPa)*	800
$\varepsilon_{uc,L}$	0.018
$S_{ut,T}$ *(MPa)*	40
$\varepsilon_{ut,T}$	0.025
$S_{uc,T}$ *(MPa)*	145
$\varepsilon_{uc,T}$	0.012
τ_u *(MPa)*	73
γ_u	0.040

The shell was modelled with the *Laminated Composite Fabric* material model of LS-DYNA. This material model is capable of predicting initiation and evolution of intra-laminar damage through degrading elastic moduli (Xiao et al. 2009). It is suitable for modelling UD and woven composites. According to this model, a UD lamina can fail under tension and compression in fibre and matrix directions and under in-plane shear (relevant parameters are given in Table 2 for the glass/epoxy lamina). The 1.3 mm thick and 20 mm wide chin strap was modelled with the *Elastic* material model. Its properties are presented in Table 1.

CAD files of the shell and liner were imported into the Hypermesh environment (HyperWorks 2008), where they were discretised. The liner was meshed with single integration 4-node tetrahedral elements. The tetrahedron is suitable for mesh generation on complicated volumes such as a helmet liner, but it is susceptible to excessively stiff behaviour (locking) (Cook 2001). Cernicchi et al. (2008) compared the impact response of a foam mat meshed with tetrahedral and hexahedral elements. They concluded that when 4–5 elements were used through the thickness, the results converged regardless of the type of the elements. Following these suggestions, the liner was meshed with 39836 elements.

The shell was meshed with 4-node shell elements. Simulation of helmet impacts onto a kerbstone anvil indicated that with shell mesh size of 3 mm, 6 mm and 10 mm, the variation of the peak head acceleration and the dissipated energy by the shell was less than 10%. Therefore, 3 mm shell element size was chosen to precisely mesh complex areas of the shell (such as its sides); the shell was meshed with 24162 elements. Each layer was represented with a through thickness integration point.

Contact was defined at the liner/head, chin strap/head, shell/liner and shell/anvil interfaces using the automatic contact algorithm with penalty formulation (Hallquist 2007b). Sliding at the interfaces was modelled using the Coulomb friction model. The friction coefficients at the shell/liner and liner/head interfaces were set to 0.5. At the shell/anvil interface, a 0.23 friction coefficient, obtained from helmeted dummy drop tests, was employed.

3. FE model of the Hybrid III dummy

The family of Hybrid III dummies has been developed by General Motors Corporation for investigating injuries of car occupants in high-speed frontal impacts. This dummy has a flexible neck made of rubber cylinders separated with aluminium

discs. Through the centre of this column runs a steel cable. The neck is attached to the head with a revolute joint (Occipital Condyle), whose axis is normal to the coronal plane. At the other end, it is rigidly attached to a rigid steel thoracic spine (the main upper part of the back).

An FE model of the dummy (LSTC.H3.103008_v1.0), which was developed by the Livermore Software Technology Corporation (LSTC), was employed in this research. This model has 7444 nodes and 4295 elements composed of 2648 solid, 1636 shell, 3 beam and 8 discrete elements. The mesh of the head's skin was very coarse compared to the mesh of the helmet liner. Using a CAD file of the skin, a finely meshed FE skin including 3704 hexahedral elements (compared to 136 elements of the original FE skin) was created. The performance of the FE model was studied and validated through simulating helmeted dummy drop tests.

4. Validation of the model of the helmeted dummy

In order to validate the FE model of the helmeted dummy, a 50th percentile male Hybrid III dummy in the sitting posture was equipped with the AGV-T2 helmet and drop tested at TRL (UK, another partner of the MYMOSA network). The helmets were size M (57-58). They were positioned on the dummy's head considering the peripheral vision requirements of UNECE 22.05 and the chin strap was fastened with a normal force. The neck of the dummy was calibrated before tests as per the FMVSS 572 (1986) standard. The dummy was dropped in a free fall from the required height to reach a speed of 6 m/s at the onset of the helmet/anvil contact. Its body axis was horizontal and the helmet impacted the flat anvil at the front site (Figure 2). The test was repeated three times; the mean of the impact velocity was 5.9 m/s and its standard deviation was ±0.1 m/s.

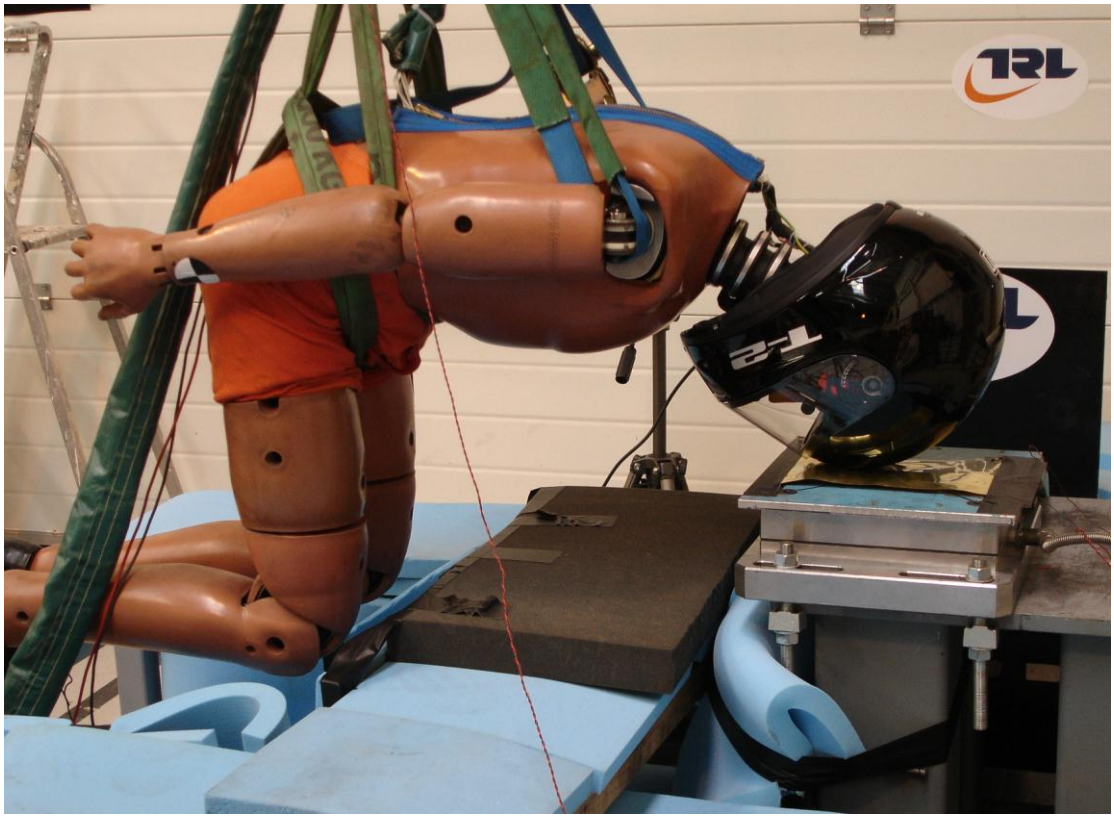

Figure 2 Helmeted dummy drop test set up.

The head of the dummy was instrumented with a nine accelerometers package (Padgaonkar et al. 1975). A standard load-cell was mounted at the Occipital Condyle joint. Another load-cell was located under the anvil to measure the normal and tangential components of the impact force. In total, 18 channels were connected to a DTS data logger. The data acquisition frequency was 38 kHz.

The same impact was simulated by using the FE model of the helmeted dummy. The experimental and numerical results were filtered with the fourth order Butterworth filter at a cut-off frequency of 1 kHz. As shown in Figure 3, there is good agreement between numerical and experimental results with respect to the head acceleration (|a|) and neck shear force. The experimental $|a|_{max}$ is 121±2 g and its FE predicted value is 134 g (11% higher). The experimental and numerical peaks of the neck shear force are respectively 1.41±0.04 N and 1.55 N (a 10% difference). The FE predicted neck axial force is quite lower, which indicates that the neck of the model of

the dummy is slightly stiff in the axial direction. The *HIC* was calculated as 675 from the FEA, which is slightly higher than the experimental results, 668±9.

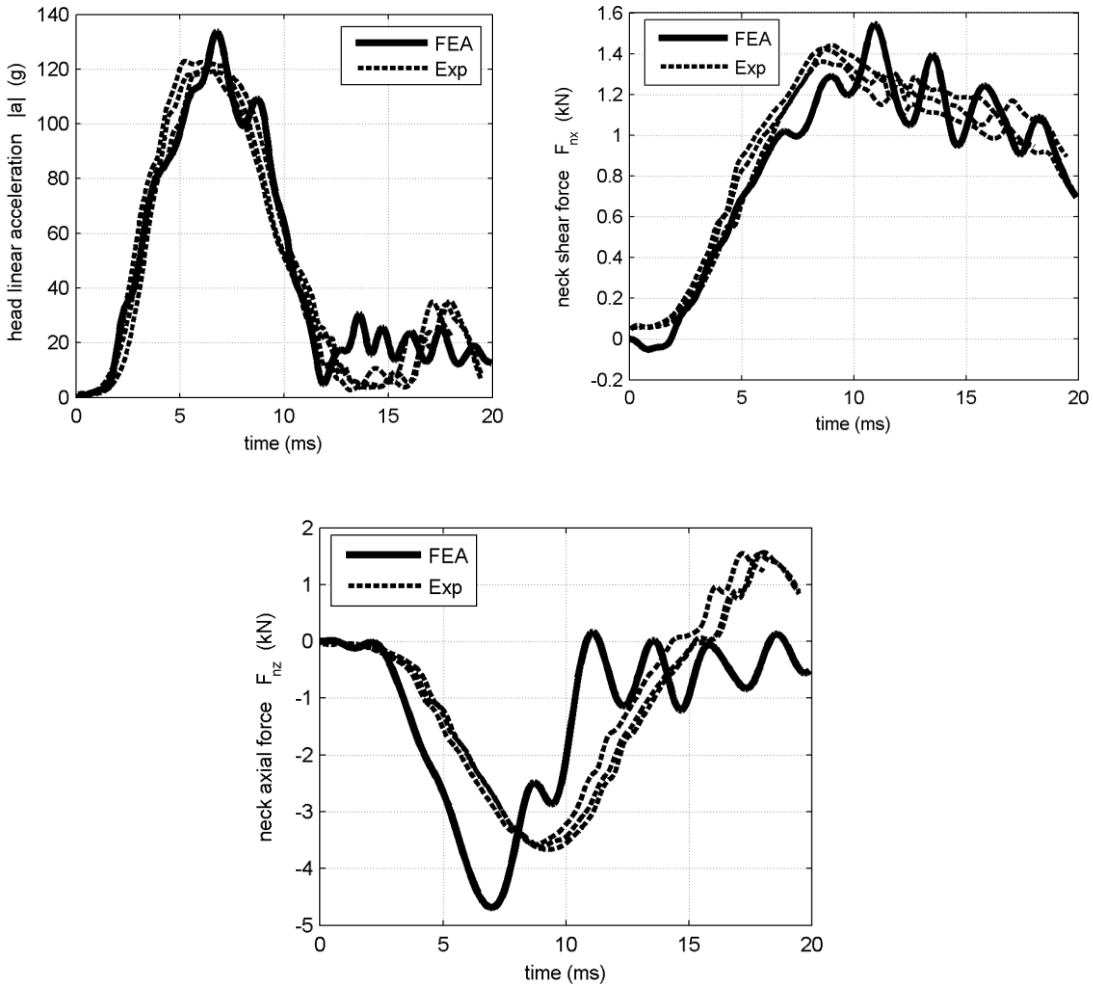

Figure 3 Results of the helmeted dummy drop tests and FEA results.

The crushing distance of the liner (Δh) is a very important impact output as it can indicate the probability of bottoming out of the liner. This parameter was not reported in previous full-body impacts. In this study, to calculate Δh, the initial clearances at the head/liner, liner/shell and shell/anvil interfaces were subtracted from the maximum displacement of the head in the direction normal to the anvil. The liner crushing distance was measured at 32±0.6 mm in experiments; its FE predicted value was 30.3 mm, which is comparable with the experimental data. In the shell at the

impact area, no damage was detected through visual inspection, which agreed with the simulation results. The above comparisons indicate that the model tends to give good predictions of the head, neck and helmet responses.

5. Full-body and detached-head drop tests

In order to reveal possible influences of the presence of the body on the impact response of the helmeted head, helmet drop tests using the Hybrid III dummy (full-body) were simulated and compared with simulations of drop tests in which only the detached head of the dummy was used. The FE model of the AGV-T2 helmet was positioned on the dummy's head and its detached head. The front edge of the helmet was displaced towards the rear by 25 mm to follow the instructions of UNECE 22.05. There was a small gap (less than 8 mm) between the head and liner, which is filled in the real helmet with the comfort liner.

The axis of the body was horizontal and the orientation of the detached head was exactly the same as the orientation of the dummy's head (Figure 4). The impact occurred at the front site. The accident investigation of COST327 showed that 43% of motorcyclists impacted the opposite object at body impact angles in the range of 0°-15°. In addition, more than 23% of the helmets were impacted in the frontal side. Therefore, the impact configuration shown in Figure 4 represents a considerable percentage of real-world accidents.

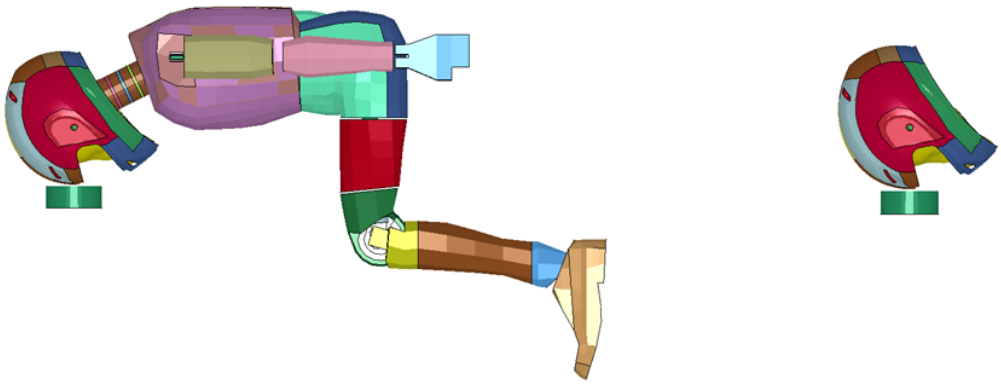

Figure 4 Helmeted Hybrid III dummy (left) and helmeted detached head of the dummy (right) impacting a flat anvil.

The dummy was in sitting posture. According to accident investigations (COST327 2001, MAIDS 2004), in motorcycle accidents the most frequent collision partners are passenger cars. In an impact with a car, the motorcyclist usually hits the car shortly after motorcycle/car collision, which means the rider does not have enough time to change posture considerably. Therefore, using a dummy in the sitting stance represents a number of body postures immediately before the impact.

The impacts were against a flat anvil at two impact velocities, 6 m/s and 7.5 m/s. The former was used in the COST study to perform the same comparison but experimentally. The latter is the velocity adopted by the UNECE 22.05 regulation.

6. Comparison between full-body and detached-head impacts

In Figure 5, $|a|$ and the helmet/head interface contact force in the direction normal to the anvil pointing towards the head (F_{hN}) are plotted for drop tests at 6 m/s. It should be noted that the front edge of the helmet was displaced towards the rear by 25 mm to comply with the instructions of UNECE 22.05, while in the experiments and corresponding simulations it was not displaced to reduce the risk of damaging the dummy due to possible head/anvil contact. As shown in this figure, F_{hN} increased as a

result of the presence of the body (but its maximum value was still less than the threshold of skull fracture, 11.9 kN, (Yoganandan et al. 1995)). Another consequence of including the body was a decrease in $|a|$, which can be related to the component of the neck force that acts on the head in the direction opposite to F_{hN}. The value of this force is probably dependent on the stiffness of the neck and the inertia of the rest of the body. The comparisons shown in Figure 5 are consistent with those reported in COST 327 for similar drop tests. However, the crushing distance of the liner was not reported in COST 327 in contrast to the current study. As reported in Table 3, Δh was larger when the dummy was used.

Table 3 Results of drop test simulations

Impact Type	V_0 (m/s)	$\|a\|_{max}$ (g)	HIC	$F_{hN,max}$ (kN)	$\Delta h_{max}/h$ *
Detached-head	6	133	597	5.5	0.64
	7.5	216	1274	8.9	0.81
Full-body	6	113	499	7.6	0.79
	7.5	278	1613	17.2	0.91
Modified Detached-head	6	123	487	7.4	0.79
	7.5	265	1523	16.0	0.91

* This quantity is an approximation of the maximum compressive strain of the liner in the crushed region (h = 42 mm).

The results of the drop tests at 7.5 m/s are plotted in Figure 6. This figure shows that in the full-body impact, $|a|$ rises suddenly after 6 ms and exceeds that of the detached head. This is in contrast to the behaviour shown in Figure 5 and that reported in previous experimental studies (Aldman et al. 1976, Aldman et al. 1978a, Aldman et al. 1978b, COST327 2001). This phenomenon is the consequence of the bottoming out of the liner. Increasing the impact speed from 6 m/s to 7.5 m/s caused more deformation of the liner such that its maximum compressive strain in the crushed region reached 91% for the dummy drop test (Table 3). As reported in Table 3, $|a|_{max}$ exceeded the limit set in the UNECE 22.05 (275 g) and $F_{hN,max}$ was far larger than the skull fracture threshold, which indicate that the energy absorption capacity of

the helmet was not sufficient for this impact. Bottoming out of the liner also increased the *HIC* as compared to the detached-head impact at 7.5 m/s, but its value was less than the limit set in UNECE 22.05.

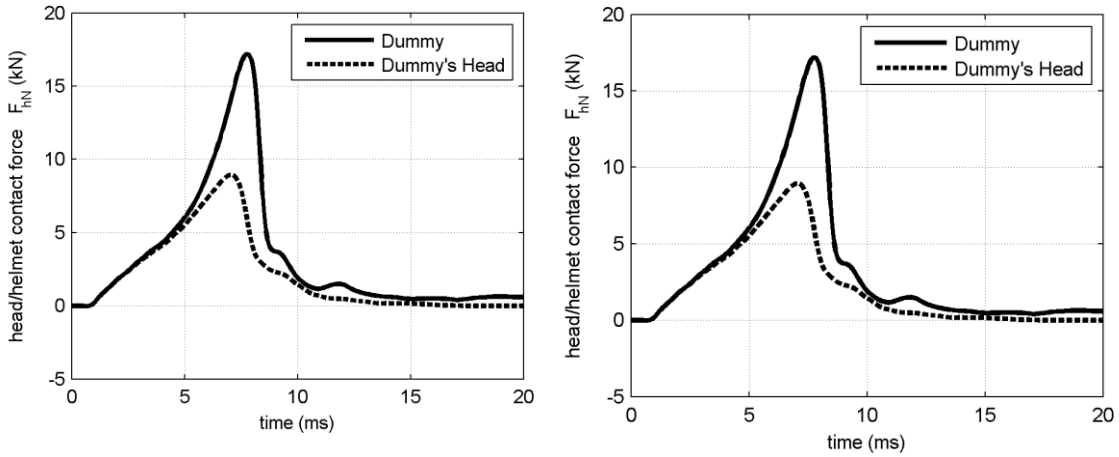

Figure 6 Results of full-body and detached-head drop tests at 7.5 m/s.

Helmet liners are usually designed to reach a maximum compressive strain, when drop tested according to standard procedures, which is not in the densification region of their stress-strain curve in order to avoid bottoming out. Current standards employ a headform in drop tests, while real-world accidents are full-body impacts; as it was shown the liner is compressed more in full-body than detached-head impacts. This implies that the current helmet standards underestimate the liner crushing distance. Now the question is how the standard test method can be modified to include the effect of the body. To answer this question, an analytical model is proposed for the standard drop test.

7. Analytical model of standard drop test

Two parts of a helmet absorb impact energy: the liner and the shell. The liner is usually made of EPS, whose typical stress-strain curve has a wide plateau region (Figure 1). Gilchrist and Mills (1994) assumed a constant yield stress (σ_Y) for the liner

under compression and derived the following relation between the normal force on the helmet (F_N) impacting a flat anvil, and the central deflection of the liner (y):

$$F_N = 2\pi\ R\sigma_Y y \tag{3}$$

The helmet was assumed to be locally spherical with radius R. For impacts onto kerbstone or spherical anvils, this radius should be replaced with an equivalent radius using the relation between equivalent curvatures (Gilchrist and Mills 1994). Eq. (3) was found to give a good approximation of the impact behaviour of thin-shelled helmets such as bicycle helmets. A function of the relatively stiff shell of motorcycle helmets is to increase the shell/liner contact area for impacts with kerbstone or spherical anvils. This effect can be taken into account by increasing R, as explained in (Gilchrist and Mills 1994).

Another function of the shell is to absorb part of the impact energy. Its contribution to energy absorption is usually 10 to 30% (Shuaeib et al. 2002), which is a considerable portion. Absorption of the kinetic energy by the shell reduces the speed of the helmet and headform. Therefore, it can be assumed that the impact of a helmet onto an anvil is equivalent to the same impact but at a reduced impact velocity when the shell is removed. To calculate the reduced impact velocity, the energy conservation principle is employed as follows:

$$\frac{1}{2}mV_0^2 = IE_{shell} + IE_{liner} \tag{4}$$

where m is the mass of the helmet and headform and IE is the internal energy (combination of the elastic energy and dissipated energy) at the instance that the velocity is zero just before rebounding. Using the ratio of the total internal energy to the internal energy of the liner (α), the above equation can be written as:

$$\frac{1}{2}mV_0^2 = \alpha IE_{liner} \tag{5}$$

or

$$IE_{liner} = \frac{1}{2} m(\frac{V_0}{\sqrt{\alpha}})^2 \quad (6)$$

Thus, the reduced impact velocity ($V_{0,r}$) is:

$$V_{0,r} = \frac{V_0}{\sqrt{\alpha}} \quad (7)$$

By replacing the impact velocity with the reduced impact velocity, the shell can be ignored in the model.

It was assumed that the liner and headform are one rigid body whose centre of gravity is located at the centre of gravity of the headform. By using Newton's second law and substituting for force from eq. (3), we have:

$$m\ddot{y} = -2\pi\ R\sigma_Y y \quad (8)$$

The earth's gravity is not considered in this equation as it is negligible compared to accelerations expected in helmet drop tests. Assuming $y(0)=0$, the solution to the differential eq. (8) is:

$$y(t) = \frac{V_{0,r}}{\omega} \sin \omega t, \quad \omega = \sqrt{\frac{2\pi R\sigma_Y}{m}} \quad (9)$$

The derivation of the peak linear acceleration of the headform (a_{max}), the maximum normal force on the anvil ($F_{N,max}$) and the maximum compression of the liner (Δh_{max}) is straightforward from eqs. (3), (8) and (9):

$$a_{\max} = \frac{V_{0,r}}{\sqrt{m}} \sqrt{2\pi R\sigma_Y} \quad (10)$$

$$F_{N,\max} = \sqrt{m} V_{0,r} \sqrt{2\pi R\sigma_Y} \quad (11)$$

$$\Delta h_{\max} = \frac{\sqrt{m} V_{0,r}}{\sqrt{2\pi R\sigma_Y}} \quad (12)$$

Head linear acceleration in eq. (10) is equivalent to $|a|_{max}$ since the model has only one translational degree of freedom.

Eqs. (10) to (12) may not be used for final design of helmets but can provide very useful information about the relation between impact inputs, main properties of the helmet and impact outputs. For example, they predict that in order to decrease acceleration of the headform by 20%, the yield stress of the foam (which is a function of its density) should be decreased by about 36%. In addition, the thickness of the liner should be increased because by decreasing σ_Y, Δh_{max} increases. These equations are used in the next section to suggest how the standard helmet drop test can be modified in order to take into account the important effect of the presence of the body.

8. Modified headform

It was shown that the presence of the whole body results in further crushing of the liner. Therefore, the body has an important effect, which should be considered in the impact absorption tests. Since using a dummy to test helmets has a drastic impact on their cost, other measures should be adopted.

The results given in Table 3 indicate that when the liner was not loaded beyond its energy absorption capacity (V_0 = 6 m/s), $|a|_{max}$ was lower in the full-body impact, but $F_{hN,max}$ and Δh_{max} were greater. Referring to eqs. (10) to (12), the only modification to the helmeted headform impact inputs that influences the outputs in the same way is increasing the mass of the headform.

The increased mass of the headform can be estimated by using Newton's second law for the rigid head of the dummy in the direction normal to the anvil, as follows:

$$F_{hN}/a_N = -F_{nN}/a_N + m_h \tag{13}$$

F_{nN} is the head/neck joint force and m_h is the mass of the head. The subscript N refers to the direction normal to the anvil pointing towards the head. $-F_{nN}/a_N$, which has a positive value in the loading phase, has the dimension of mass. It can be interpreted as

a mass that should be added to the mass of the head if the rest of the body is removed in order to maintain F_{hN}/a_N at the same level. In other words, $-F_{nN}/a_N$ is the contribution of the body through the neck to generating higher F_{hN}/a_N. $-F_{nN}/(m_h\, a_N)$, a dimensionless parameter, is the ratio of the added mass to the mass of the head, which will be denoted by γ_m. This parameter, called the "added mass index", can be used to evaluate the influence of the body through the neck on $|a|_{max}$, $F_{hN,max}$ and Δh_{max}.

Figure 7 plots γ_m for the helmeted Hybrid III dummy virtual drop test at 7.5 m/s. As shown in this figure, γ_m is not constant during the impact. It varies gradually until the peak acceleration occurs. Then, it increases with a steep slope as acceleration falls towards zero. As the aim was to include the body effect on $|a|_{max}$, $F_{hN,max}$ and Δh_{max}, which occur at approximately the same time, the value of γ_m at the peak head acceleration, 0.43, was chosen to calculate an increased mass for the detached head of the dummy. The detached head of the dummy was modified by increasing its mass by $\gamma_m = 0.43$, and it was virtual drop tested with the helmet in the same impact conditions.

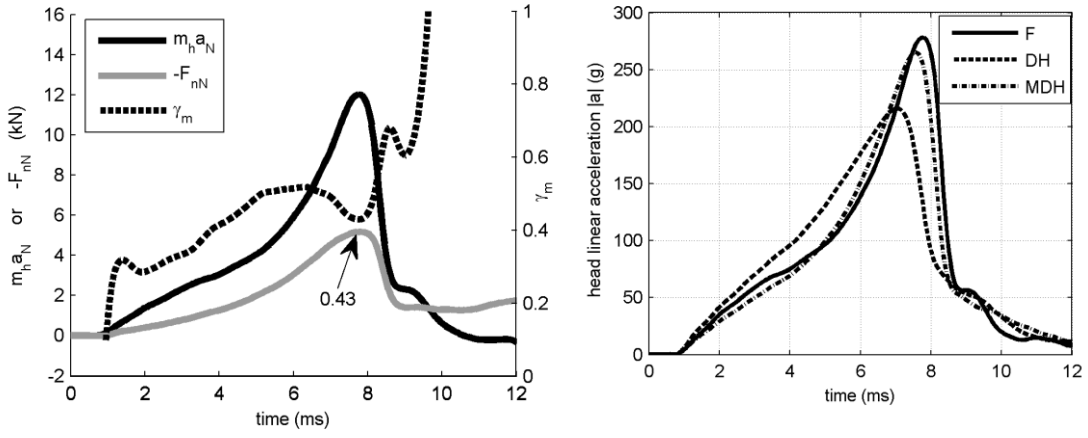

Figure 7 Added mass index for the helmeted dummy drop test (left) and comparison of the results using γ_m=0.43 (right); at a 7.5 m/s impact velocity; F: full-body, DH: detached-head and MDH: modified detached head.

Figure 7 compares $|a|$ between the full-body, modified detached-head and detached-head drop tests. The head acceleration curve obtained from the modified detached-head drop test compares well with that of the dummy drop test, which is remarkable because it is acknowledged that both the acceleration level and its dwell time are indicators of head injury. As a result, *HIC*, which is a function of linear acceleration vs. time, was predicted with a less than 6% error as presented in Table 3. $F_{hN,max}$, which is an indicator of skull fracture, was also predicted precisely using the modified detached head. The maximum crushing distance of the liner, Δh_{max}, was also replicated successfully. Therefore, a suitable value was selected for the added mass index for the given impact conditions.

9. Discussion

The FE model of the helmeted Hybrid III dummy was validated against experimental data with respect to the head linear acceleration and neck forces. Then, it was used to simulate full-body helmet drop tests. The results were compared to the results of the same impacts but by using the detached head of the dummy. It was shown that including the whole body in the impacts reduced $|a|_{max}$ when the foam liner at the crushed region did not enter the densification region of its characteristic stress-strain curve, but it increased $F_{hN,max}$ and $\Delta h_{,max}$. These results are similar to the experimental findings reported in COST (2001) for an impact velocity of 6 m/s, except for the crushing distance of the liner, which was not reported in that reference. As shown in this work, an increase in the impact velocity from 6 m/s to 7.5 m/s caused bottoming out of the liner in the full-body impact and consequently a very high contact force and head acceleration. These results raise doubts about helmet testing procedures prescribed by standards, which employ a headform.

Using a dummy to drop test helmets would be cumbersome and would have a drastic impact on their cost. A simple and economical way of including the effect of the body in drop tests is to use a headform but to change one (or more) impact conditions. The closed-form equations suggested that increasing the mass of the headform can replicate the influence of the body on $|a|_{max}$, $F_{hN,max}$ and particularly $\Delta h_{,max}$. The comparison between the results of drop tests using the dummy and its detached head modified by increasing its mass confirmed this hypothesis. The increased mass was obtained for an impact configuration frequent in real world accidents. More impact configurations have been investigated in (Ghajari 2010).

Using a heavier headform with the same limit of head linear acceleration can cause helmet manufacturers to use foams with higher yield stress (stiffer); a conclusion that can easily be drawn from eq. (10). However, in real-world impact conditions the head might virtually decouple from the body, for instance when the body is stopped by an obstacle before the head impacts another object. Consequently, a helmet that has passed the new test method may induce higher head decelerations due to its stiffer liner as compared to a helmet approved by current standard tests, such as those of UNECE 22.05. Consider a helmet that has been designed to pass the new test method so that peak headform acceleration is equal to the injury limit of head acceleration (A). For this helmet, from eq. (10), we have:

$$A = \frac{V_{0,r}}{\sqrt{(1+\gamma_m)m_h + m_{helmet}}} \sqrt{2\pi R \sigma_Y} \qquad (14)$$

In impact conditions where the head decouples from the body, γ_m is zero. If the impact speed and site are the same as those of the standard test, the right hand side of the above equation would become larger than A. To avoid such a design, the head linear acceleration limit set in the standard should be decreased to:

$$A' = A \Big/ \sqrt{\frac{(1+\gamma_m)m_h + m_{helmet}}{m_h + m_{helmet}}} \tag{15}$$

With this correction, the new design of the helmet has to satisfy the following equation:

$$A = \frac{V_{0,r}}{\sqrt{m_h + m_{helmet}}} \sqrt{2\pi R \sigma_Y} \tag{16}$$

where γ_m is not involved anymore. The limit of acceleration should be reduced the most when $m_{helmet} << m_h$, which results in $A' = A/(1+\gamma_m)^{0.5}$. For $\gamma_m = 0.43$, $A' = 0.84A$.

The value obtained for γ_m was based on using the Hybrid III dummy as a surrogate for the human body. This dummy was developed to study car frontal impacts, in which the head is under indirect loading. Some researchers believe that it is not suitable for investigating direct impacts to the head, such as motorcycle accidents, because its neck is too stiff in the axial direction (Herbst et al. 1998). A new dummy neck with improved biofidelity (Withnall and Fournier 1998) has been designed to replace the modified Hybrid III neck used in an early version of ISO 13232. This neck addresses the posture and multi-directional biofidelity required for motorcyclist anthropomorphic test devices. In sled tests (Withnall et al. 2003), its response compared to volunteer test corridors was better than the response of the Hybrid III neck. However, no study was found in literature that has investigated its biofidelity under direct impact loading, such as in inverted drop tests. Therefore, the Hybrid III neck was employed in this work as its behaviour under direct loading has been addressed in several studies (Frechede et al. 2009, Herbst, Forrest, Chng and A. Sances 1998, Sances et al. 2002); in addition, it was available within the consortium. Using human body surrogates whose neck can better reproduce the behaviour of the human neck under axial loading would probably modify the calculated value of γ_m, but would not modify its concept, which is the main idea of the present paper.

In this study, the rotational acceleration of the head was not evaluated. A previous study concluded that the most effective countermeasure of reducing the head rotational acceleration could be mitigating the head linear acceleration (Mills et al. 2009). Therefore, modifying the headform mass, in order to avoid high linear accelerations due to helmet bottoming out, can also decrease the probable high rotational accelerations triggered by the same phenomenon.

Finally, the concept of the added mass index, γ_m, has been presented here with reference to only one impact configuration. A much wider investigation has been carried out in (Ghajari 2010), where the influence of different impact configurations and various models of the human body on the value of the mass index are taken into account.

10. Conclusions

A commercially available helmet was drop tested virtually by using validated FE models of the Hybrid III dummy and its detached head. It was shown that the presence of the body increases the liner crushing distance. This effect caused complete bottoming out of the liner at an impact speed of 7.5 m/s and consequently the large head acceleration and contact force. Using the solution to an analytical model of the helmet drop test and FEA results, it has been shown that increasing the mass of the headform can be a simple yet appropriate way of including the effect of the whole body in drop tests. A dimensionless parameter (γ_m) called the added mass index has been defined, which is the ratio of the proposed increase in the headform mass to its original mass. This index quantifies the effect of the body on the impact response of the helmeted head. If the mass of the headform is to be increased by γ_m, the limit of head acceleration set in the standard should be decreased by $(1+\gamma_m)^{0.5}$ in order to avoid the design of helmets which have too stiff liners.

Acknowledgements

The work presented in this paper was completed within the research training network MYMOSA funded by a Marie Curie fellowship of the 6th framework programme of the EU under contract no. MRTN-CT-2006-035965. The authors would like to thank Dainese S.p.A. for providing the AGV-T2 helmets. TRL is also to be thanked for providing the Hybrid III dummy, test facilities and technical assistance for performing the dummy drop tests.

References

ACEM. 2006. ACEM's view on PTW fatality statistics in Europe. Belgium.
Agarwal BD, Broutman LJ and Chandrashekhara K. 2006. Analysis and performance of fiber composites. 3rd ed. Hoboken, N.J.: John Wiley.
Aldman B, Lundell B and Thorngren L. 1976. Non-perpendicular impacts, an experimental study on crash helmets. In. IRCOBI; 1976.
Aldman B, Lundell B and Thorngren L. 1978a. Helmet attenuation of the head response in oblique impacts to the ground. In. IRCOBI; 1978a.
Aldman B, Lundell B and Thorngren L. 1978b. Oblique impacts, a parametric study in crash helmets. In. IRCOBI; 1978b.
Becker EB. 1998. Helmet development and standards. IOS Press.
Cernicchi A, Galvanetto U and Iannucci L. 2008. Virtual modelling of safety helmets: practical problems. International Journal of Crashworthiness. 13(4):451-467. Available from <Go to ISI>://000257472900008 DOI 10.1080/13588260802055460
Cook RD. 2001. Concepts and applications of finite element analysis. 4th ed. New York, NY: Wiley.
COST327. 2001. Motorcycle safety helmets, final report of the action. Belgium.
Di Landro L, Sala G and Olivieri D. 2002. Deformation mechanisms and energy absorption of polystyrene foams for protective helmets. Journal of Polymer Testing. 21(2):217-228. Available from <Go to ISI>://000173005300018
FMVSS572. 1986. Subpart E - Hybrid III test dummy. In: Federal Motor Vehicle Safety Standards USA.
Frechede B, McIntosh A, Grzebieta R and Bambach M. 2009. Hybrid III ATD in Inverted Impacts: Influence of Impact Angle on Neck Injury Risk Assessment. Annals of Biomedical Engineering. 37(7):1403-1414. Available from <Go to ISI>://000266643000014 DOI 10.1007/s10439-009-9711-4
Ghajari M. 2010. The influence of the body on the response of the helmeted head during impact [Ph.D. dissertation]. London: Imperial College London.
Ghajari M, Caserta GD and Galvanetto U. 2008. Comparison of safety helmet testing standards. London: MYMOSA EU research training network.
Gibson LJ and Ashby MF. 1999. Cellular solids. Cambridge University Press.
Gilchrist A and Mills NJ. 1994. Modeling of the Impact Response of Motorcycle Helmets. International Journal of Impact Engineering. 15(3):201-218. Available from <Go to ISI>://A1994NR70700002
Gilchrist A and Mills NJ. 1996. Protection of the side of the head. Journal of Accident Analysis and Prevention. 28(4):525-535. Available from <Go to ISI>://A1996VE55200013
Hallquist JO. 2007a. Ls-Dyna keyword user's manual: Livermore software technology corporation.
Hallquist JO. 2007b. Ls-Dyna theory manual: Livermore software technology corporation.

Herbst B, Forrest S, Chng D and A. Sances J. Fidelity of anthropometric test dummy necks in rollover accidents. In. 16th International Technical Conference on the Enhanced Safety of Vehicles; Windsor, Canada.
HIC-Workshop. Final report of workshop on criteria for head injury and helmet standards. Milwaukee.
HyperWorks. 2008. Release 9.0: Altair.
Kleiven S. 2006. Evaluation of head injury criteria using a finite element model validated against experiments on localized brain motion, intracerebral acceleration, and intracranial pressure. International Journal of Crashworthiness. 11(1):65-79. Available from <Go to ISI>://000236797000006 DOI 10.1533/ijcr.2005.0384
Livermore software technology corporation: www.lstc.com
MAIDS. 2004. MAIDS final report 1.2: in-depth investigations of accidents involving powered two wheelers. Belgium.
Mills NJ and Gilchrist A. 2008. Finite-element analysis of bicycle helmet oblique impacts. International Journal of Impact Engineering. 35(9):1087-1101. Available from <Go to ISI>://000257096800013 DOI 10.1016/j.ijimpeng.2007.05.006
Mills NJ, Wilkes S, Derler S and Flisch A. 2009. FEA of oblique impact tests on a motorcycle helmet. International Journal of Impact Engineering. 36(7):913-925. Available from <Go to ISI>://000264973300004 DOI 10.1016/j.ijimpeng.2008.12.011
Padgaonkar AJ, Krieger KW and King AI. 1975. Measurement of angular acceleration of a rigid body using linear accelerometers. Journal of Applied Mechanics -Transactions of the ASME. 42(3):552-556. Available from <Go to ISI>://A1975AQ74900005
Sances A, Carlin F and Kumaresan S. 2002. Biomechanical analysis of head-neck force in hybrid III dummy during inverted vertical drops. Biomedical Sciences Instrumentation, Vol 38. 38:459-464. Available from <Go to ISI>://000184842900077
Shuaeib FM, Hamouda AMS, Hamdan MM, Umar RSR and Hashmi MSJ. 2002. Motorcycle helmet - Part II. Materials and design issues. Journal of Materials Processing Technology. 123(3):422-431. Available from <Go to ISI>://000176486200014 Pii S0924-0136(02)00047-X
Tinard V, Deck C, Meyer F, Bourdet N and Willinger R. 2009. Influence of pedestrian head surrogate and boundary conditions on head injury risk prediction. International Journal of Crashworthiness. 14(3):259-268. Available from <Go to ISI>://000267822700004 Doi 10.1080/13588260802434046
Pii 912992761
UNECE22.05. 2002. Uniform provisions concerning the approval of protective helmets and of their visors for drivers and passengers United Nations.
Withnall C and Fournier E. 1998. A new neck for motorcycle crash testing. In. 16th international technical conference on the enhanced safety of vehicles; 1998; Windsor, Canada.
Withnall C, Schewchenko N, Wiley KD and Rogers N. 2003. An improved dummy neck for the ISO 13232 motorcycle anthropometric test dummy. In. 18th international technical conference on the enhanced safety of vehicles; 2003; Nagoya, Japan.
Xiao XR, Botkin ME and Johnson NL. 2009. Axial crush simulation of braided carbon tubes using MAT58 in LS-DYNA. J Thin-Walled Structures. 47(6-7):740-749. Available from <Go to ISI>://000265894800013 DOI 10.1016/j.tws.2008.12.004

Yoganandan N, Pintar FA, Sances A, Walsh PR, Ewing CL, Thomas DJ and Snyder RG. 1995. Biomechanics of skull fracture. Journal of Neurotrauma. 12(4):659-668. Available from <Go to ISI>://A1995RY92000017